Atomic Force Microscopy Visualization of Morphology Changes Resulting from the Phase Transitions in Poly(di-*n*-alkylsiloxane)s: Poly(diethylsiloxane)

Yuli K. Godovsky

Karpov Institute of Physical Chemistry, 10 Vorontsovo Pole, 103064 Moscow, Russia

Vladimir S. Papkov

Nesmeyanov Institute of Organoelement Compounds, Russian Academy of Sciences, 28 Vavilov Str., 117813 Moscow, Russia

Sergei N. Magonov*

Digital Instruments/Veeco Metrology Group, 112 Robin Hill Rd., Santa Barbara, California 93117

Received May 16, 2000; Revised Manuscript Received October 6, 2000

ABSTRACT: The results of visualization of morphology and nanostructure of polydiethylsiloxane (PDES) are presented. The study was performed in a temperature range, which covers melting, crystallization, mesophase formation, and isotropization of PDES, on polymer samples of different molecular weights and different thicknesses. The morphological identification of α_2- and β_2-polymorphs of PDES was further extended by demonstrating, for the first time, that the α_2- and β_2-crystalline polymorphs transform to two morphologically incompatible α-mesophase and β-mesophase. Domains, which are several microns in size, are typical morphologic patterns for the α-phase material, whereas large lamellae (from a few to tens of microns in length and several hundreds of nanometers in width) are typical structures of the β-phase PDES. The above polymorphs and amorphous polymers have appeared in different ratios in the samples depending on their preparation (deposition way, thermal history) and thickness. Shearing of PDES into thin film on Si substrate induced the formation of the mesomorphic β-phase structures, which are embedded in amorphous material. Crystallization of the amorphous PDES occurred at much lower temperatures due to its constrained geometry. The width of the β-phase lamellae in the crystalline and mesomorphic state as measured from AFM images correlates with the length of the extended PDES chains in the crystalline state. Sublamellae structures were revealed by AFM imaging the mesomorphic lamellae with different tip−sample forces. Each lamella has a skeleton formed of 10−15 nm thick linear structures, which are separated by 40−50 nm and tapered at the ends to form a single entity. This skeleton is wrapped with numerous 0.8 nm thick layers, which are most likely formed of partially ordered domains of extended chains. Crystallization of the β-mesomorphic lamellae leads to more ordered and stiffer top layers of lamellae. In some cases individual lamellae are broken into small crystalline blocks, and in other cases crystalline blocks incorporate two neighboring lamellae. The domains of the mesomorphic α-phase are less organized, and upon crystallization large domains are broken into smaller blocks due to shrinkage. This is accompanied by surface roughening. Some of the blocks exhibit periodic surface structures with a repeat distance of 50−60 nm. At least partial chain extension in the α-phase PDES is suggested.

Introduction

Poly(di-*n*-alkylsiloxane)s with ethyl to hexyl side chains are nonpolar flexible macromolecules exhibiting polymorphism and mesomorphism.[1,2] Two crystalline forms, which are known as α- and β-forms, exist in high- and low-temperature modifications. At higher temperatures, the crystals of the poly(di-*n*-alkylsiloxane)s transform into a mesophase in which extended macromolecules are arranged into a two-dimensional quasi-hexagonal lattice without a long-range order along the chain direction.[1,2] This arrangement, which was also considered as a conformationally disordered phase,[3,4] resembles columnar discotic phases formed in a number of liquid crystalline polymers.[5] Although this structural similarity is unexpected, because the poly(di-*n*-alkylsiloxane)s do not have mesogenic groups, it is widely accepted now.

Poly(diethylsiloxane) (PDES) is examined in more detail than other homologues, and a phase diagram of this polymer in Figure 1 demonstrates its polymorphism and mesomorphism. The mesomorphic PDES could be

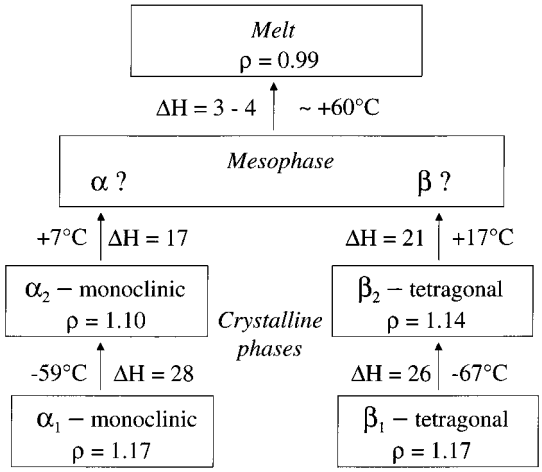

Figure 1. Phase diagram of PDES. ρ = density (g/cm^3), ΔH = heat of transition (J/g).

* Author for correspondence. E-mail sergei@di.com.

10.1021/ma000845v CCC: $20.00
Published on Web 01/05/2001

obtained either on slow cooling of the melt or by melting of crystalline polymorphs. X-ray[6] and DSC[7] studies showed that slow cooling of the melt leads to the formation of the columnar mesophase, which on further cooling transforms into crystalline β-PDES. This polymorph is thermodynamically more stable than crystalline α-PDES, which is formed after quenching of the melt. Cooling of the melt at an intermediate rate results in a mixture of α- and β-forms, and this is a most common practice. The structural incompatibility of these forms does not allow α-crystal to β-crystal transformations. Heating of α-PDES and β-PDES transforms the polymer to the mesophase, which so far was considered as identical for both crystalline polymorphs. Temperature stability of the mesophase depends strongly on the molecular weight of the poly(di-*n*-alkylsiloxane),[1,2] and the mesophase forms only for PDES with molecular weight over 28K.[8,9]

The discovery of the mesophase in PDES in 1975[10−12] stimulated characterization of this polymer by DSC, optical and electron microscopy, X-ray diffraction, NMR, and other techniques in order to understand the mesophase structure and its relation to the crystalline polymorphs.[13−28] The crystal−mesophase transition observed on heating at sub-RT temperatures gives samples with almost 100% mesophase content.[6−8,13,19,27] The comparison of the PDES density in the mesophase with the theoretical crystallographic density showed[7] that the chain packing in this phase can be described by a monoclinic unit cell, which slightly differs from the hexagonal packing. Polarized optical microscopy revealed a formation of extended lamellar structures in the mesophase obtained by slow cooling of the melt.[17] The extended lamellae or their aggregates, which are up to a few microns in width and tens of microns in length, have been seen immersed in a nonstructured matrix. The polarization contrast of these structures led to an assumption that PDES chains are lying parallel to the surface and being extended in the short dimension.

This was first but not the only result that led to a suggestion about an extended conformation of PDES chains in the mesophase. Neutron scattering experiments and computer modeling[26] provided an independent support of this idea. Electron microscopy studies of PDES morphology on freeze-fractured surfaces of bulk samples revealed the crystalline lamellae and aggregates of mesomorphic lamellae.[8,9,32] These structures are 50−3000 nm thick depending on their thermal history and molecular weight. Spherulites, which are a common crystalline morphology of flexible polymers, were not observed in the bulk crystalline PDES. Similarity of the PDES morphology to that of PE crystallized under high pressure[29−31] further strengthened the concept of extended chain conformation in the crystalline and mesomorphic phases of PDES. An unusually high degree of crystallinity is a common feature of all these samples. There are two important reasons for the development of the lamellae with the extended chain conformation in the PDES mesophase. First, the large (hundreds of nanometers) transverse dimensions of the primary and secondary nuclei for the formation of the lamellae resulting from the low enthalpy of isotropization (Figure 1). Second, the high level of molecular mobility in the mesophase, which was detected with NMR, promotes further thickening and perfection of these lamellae during and after their growth.

Table 1. Characteristics of PDES

sample	M_n	M_w	M_w/M_n	$T_{\alpha\to\mu}$ (°C)	$T_{\beta\to\mu}$ (°C)	$T_{\mu\to i}$ (°C)	T_g (°C)
PDES-1	95 300	162 000	1.71	7	17	47	−139
PDES-2	430 000	596 000	1.39	8	17	51	−139

Despite the fact that the main concept of structural organization of PDES has been worked out, there are a number of questions to be clarified. Most of them are related to the structural organization of unusually large lamellae or their aggregates. Electron microscopy studies were not able to reveal the structure of the individual mesomorphic lamellae because of their softness. Most of the structural data were obtained on samples of β-PDES, whereas the morphology of α-PDES was less examined. The chain-folded morphology was initially proposed for the crystalline α-PDES,[20] which was, however, rejected recently.[8] Instead, it was proposed that a less ordered crystalline structure of α-PDES be formed due to an incorporation of chain ends inside the crystals which prevents the formation of well-shaped lamellae.[8] Again, no distinction was suggested between mesomorphic phases obtained from crystalline α_2- and β_2-PDES.

Atomic force microscopy (AFM) has become a powerful technique for studies of polymer morphology and nanostructure.[33,34] Recently, AFM was used for characterization of the surface morphology of thin oriented layers of poly(di-*n*-alkylsiloxane)s at different temperatures.[35−37] These studies were performed in tapping mode, and the material-related contrast of phase images provides a distinctive visualization of crystalline, mesomorphic and amorphous components in PDES, and poly(dipropylsiloxane) (PDPS) samples.

In this paper we are presenting new results obtained in AFM studies of PDES, which were performed in the −50 to +52 °C temperature range on samples of different molecular weight and of different thickness (from hundreds of nanometers to several microns). The visualization of morphology and nanostructure of PDES in α_2- and β_2-crystallographic modifications and morphology changes accompanying crystallization, melting, and isotropization is reported. These results allow the addressing of the difference in morphology of α- and β-PDES not only in the crystalline state but also in the mesomorphic state. The dependence of morphology on the thermal history and sample thickness, an identification of single mesomorphic lamellae in β-PDES, and the correlation of its thickness with molecular weight were also established. Furthermore, AFM imaging at different forces reveals nanometer-scale features of individual lamellae in the mesomorphic and crystalline β-phases.

Experimental Section

Materials. The study was performed using two samples of PDES with the characteristics listed in Table 1. The samples were prepared by the anionic ring-opening polymerization of their cyclic trimers described elsewhere.[6,8,9,26] PDES-1 was the same sample, which was also examined earlier.[6,7,17,35] PDES-2 sample was synthesized in the group of Prof. M. Moeller (Ulm University, Germany) and kindly supplied to us by Dr. E. Sautter. Phase transitions in PDES were examined with a DSC-7 calorimeter (Perkin-Elmer) using 20, 10, 5, and 2 °C/min heating rates. Transition temperatures in Table 1 are given as extrapolated to zero heating rates.

For AFM investigations samples of PDES were deposited on bare Si wafer pieces. For preparation of thick layer (150 μm), the polymer was evenly spread on a hydrophobic Si surface with an applicator at 80 °C when the material was in

an isotropic molten state. To obtain various initial mesomorphic morphologies, the molten layers were either slowly cooled to room temperature or quenched in liquid nitrogen and returned to the room temperature. Thin PDES films were prepared by rubbing a piece of mesomorphic material on a plasma-treated Si surface. This treatment, which makes the Si surface hydrophilic, improves the wetting of the substrate by PDES. In earlier experiments, thin films were prepared by rubbing on a nontreated Si substrate.[35,37]

The morphology of PDES layers of various thicknesses was studied in the temperature range −50 to +52 °C, covering the temperature range from the high-temperature crystalline modifications to the melt (Figure 1).

AFM Measurements. AFM studies were performed with a Nanoscope IIIa MultiMode scanning probe microscope (Digital Instruments, Santa Barbara, CA). The results were obtained in tapping mode AFM, which is the most suitable imaging technique for soft materials. Height and phase images were simultaneously collected on surface areas from 100 to 1−2 μm on the side. The numbers at the bottom of the images indicate the size of the scanned areas. Height images reveal surface corrugations and morphologic patterns of the polymer samples. Phase images are sensitive to minor surface features (such as steps or edges); therefore, they emphasize structural details, which are barely seen in height images. Both height and especially phase images allow visualization of different components in heterogeneous polymer systems that is usually achieved in imaging with elevated tip−sample force interactions. The advantages of phase imaging in AFM studies of PDES have been already demonstrated.[35,37] Ordered structures of crystalline and mesomorphic PDES exhibit a drastically different contrast than amorphous polymers in phase images. In general, the contrast of the phase images is related to energy dissipation in the tip−sample junction, and in many cases, it correlates with different stiffness and density of individual components of heterogeneous polymer systems. Because of the way the phase changes are recorded in the AFM instrument and of the particular experimental parameters, the same structures, say lamellae, might exhibit different phase contrast with respect to amorphous surrounding. In such cases, a shape of the surface structures helps their identification.

AFM imaging of PDES samples was performed according to the following experimental protocol. Etched Si probes (220 μm in length, resonant frequency in the 150−200 kHz range, stiffness ca. 40 N/m) were applied in all experiments. The driving frequency in tapping mode was chosen at the resonant frequency of the free-oscillating cantilever in the immediate vicinity of the sample surface. The amplitude of the free-oscillating cantilever, A_0, was typically in the 50−100 nm range. When it was possible, imaging was conducted in the *light tapping* regime (i.e., with set-point amplitude close to A_0). The set-point amplitude, A_{sp}, is 0.8−0.9 A_0 for *light tapping* and 0.4−0.5 A_0 for *hard tapping*. *Light tapping* was used for high-resolution imaging of top surface structures of individual lamellae. Visualization of amorphous, mesophase, and crystalline regions was typically achieved in phase images obtained in *hard tapping*. The differences in the mechanical properties of sample regions or components lead to different contrasts in the phase images.[34]

AFM measurements at elevated temperatures were performed with a thermal accessory designed for a Nanoscope microscope. This accessory includes a ceramic block with an embedded Pt heater, which is positioned underneath a sample puck of 0.6 cm in diameter. The sample was fixed on the puck with small traces of epoxy and with a metallic clamp from above. The metallic clamp contains a thermocouple, which touches the sample surface close to the scanning area and measures the sample temperature. The latter is recorded by an electronic control unit, which is used for powering the heater. In such a way, one can heat a sample to the temperature of interest and keep it constant with an accuracy of ±0.1 °C. For low-temperature studies, the microscope was placed in a thermoelectric chamber which was purged with liquid nitrogen. The system enabled us to cool the microscope to $T =$ −50 °C with various cooling rates and to keep it at the desired temperature with an accuracy of about ±0.3 °C.

Recording of AFM images at particular temperatures takes from several minutes up to an hour, especially when imaging at different scales and at various levels of tip−sample interactions. Also, temperature changes lead to a shift of the resonant frequency of the Si cantilever, making it necessary to retune the driving frequency. Temperature variations caused a shift of the probe position with respect to the surface region of interest because of expansion/contraction of the different components of the microscope and sample. Therefore, the vertical position of the sample with respect to the piezo-scanner was adjusted. When temperature increments were small (<5 °C), this was done with the stepper motor. When temperature increments were larger, the tip was completely withdrawn from the surface, and reengagement was performed after the sample temperature stabilized. As a result of thermal drift and reengagement, the probe might shift 1−2 μm away from the place it was imaging before. To follow temperature-induced structural changes of the same sample region, large areas (typically 15−20 μm on side) were imaged.

Results and Discussion

AFM imaging PDES-1 and PDES-2 samples at different temperatures was aimed at the visualization of their mesomorphic and crystalline structures for α_2- and β_2-phases. Results of these studies are presented in several parts. At the beginning, we discuss images of the bulk polymer samples, which were first quenched in liquid nitrogen and then recrystallized in the temperature range from −20 to −10 °C and afterward slowly heated to RT. In this way, the recrystallization of PDES leads to the crystalline β_2-phase that becomes mesomorphic at RT. We suggest that this mesomorphic state is specific for the β_2-phase. AFM images obtained from bulk samples, which were prepared by slow cooling (1 °C/min) from a molten state ($T = 100$ °C) to RT, are discussed in the main part of the paper. Slow cooled samples in the mesomorphic state should have elements of both the α- and β-PDES. Finally, AFM images of thick and thin polymer layers, which were deposited on a Si substrate by rubbing, are analyzed. Such layers have been examined with AFM,[35] yet the detailed assignment of their structures has not been done.

A. Morphology of the α- and β-PDES in Bulk Crystalline and Mesomorphic States. 1. Quenched PDES. Ambient-condition height and phase images of the bulk PDES-2 sample, which was prepared by quenching, are shown in parts a and b of Figure 2, respectively. Numerous elongated structures, which are seen in both images, dominate the morphology of this sample. They resemble large lamellae seen in optical micrographs but have smaller dimensions. The length of these small lamellae is from submicrons to a few microns, and the average width is ∼170 nm. Similar in shape but narrow platelets (width ∼ 100 nm) were observed in samples of PDES-1, which were prepared in the same way. Surface corrugations relevant to individual lamellae are in the 0−15 nm range, and their surfaces are very smooth. The sharp contrast between the lamellae and their surroundings in the phase image (Figure 2b) indicates that these mesomorphic structures are stiffer than their neighborhood. Most likely, the latter consists of amorphous polymer and some round-shaped domains, which are seen elevated in the height image. The lamellae present the most ordered part of the PDES-2 at RT, and they can be assigned to the mesomorphic β-phase.[17] Then we assume that the round-shaped domains seen in some places represent

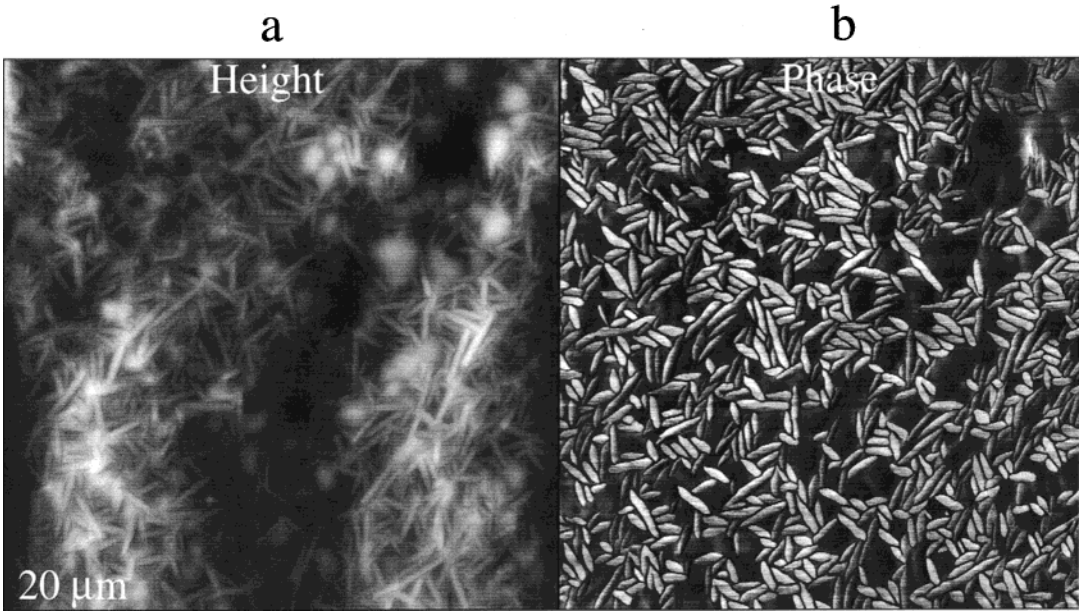

Figure 2. AFM height and phase images of a surface of bulk PDES-2 sample after quenching from a molten state in liquid nitrogen with subsequent heating to RT. Images were recorded at RT. The contrast in the height image covers the surface corrugations in the 0−120 nm range.

mesomorphic α-PDES. This assumption is reasonable because such domains became crystalline on cooling as seen below (see discussion of the images in Figures 3a−c and 4a−c). Hence, the images show that two morphologically different mesomorphic structures coexist in the sample.

Structural changes, which are observed on cooling of the quenched PDES-2 samples, support our assignment of the lamellae to the mesomorphic β-phase. The β-mesomorphic lamellae, which are seen dark in the phase in Figure 3a, transformed to crystalline lamellae of a similar shape (Figure 3b). The whole area is covered by crystalline structures with no traces of amorphous material. The crystalline lamellae are wider than their mesomorphic precursors. An increase of the lamellae width from ∼200 to ∼300 nm can be explained by an incorporation of the amorphous material into crystalline structures during crystallization. A few round-shaped α-PDES domains, which have dark contrast in the image in Figure 3a, have also crystallized and kept their shape. One of such domains surrounded by crystalline lamellae is shown in Figure 3c. We assume that this domain with a grainy nanostructure presents the crystalline α_2-phase. High-magnification images in Figure 3c,d show that the crystalline lamellae have a complex nanostructure. Nanometer-scale striations, which are seen on the surface of the crystalline lamellae, form crosshatched patterns. The repeat distance between striations oriented along the main platelet direction is ∼25 nm. Structures oriented in the perpendicular direction are generally broader but do not exhibit a well-defined pitch. The surface of the mesomorphic lamellae exhibits some strips, which are aligned perpendicular to the main direction (Figure 3a). This and other nanoscale structures of the mesomorphic lamellae will be considered below.

2. Slowly Cooled PDES. The surface morphology of the bulk PDES-2 sample, which was melted and slowly cooled to RT, is shown in Figure 4a. The phase image reveals three structural components in the sample. Extended lamellae of 250−350 nm in width and from 1 μm to tens of microns in length resemble the mesomorphic lamellae of the quenched PDES-2 samples and can be assigned to the mesomorphic β-phase. Several lamellae, which are merged together, form an 800 nm wide structure, which extends from the image top to the image bottom (see left part of the image). In contrast to the quenched PDES-2 samples, the lamellae of the mesomorphic β-phase are not the dominant structures of this sample. Surface areas surrounding the lamellae in Figure 4a exhibit different phase contrasts and can be assigned to amorphous (molten) material (bright regions) and to the mesomorphic α-phase (dark domains). Cooling of the sample from RT to $T = -15$ °C induced its crystallization. As a result, the lamellae became wider and split into a number of crystalline blocks with sharp borders (Figure 4b). The lamellae, which are very smooth structures in the mesomorphic phase, became rough after crystallization. The rest of the crystallized polymer consists of a large number of domains that could be assigned to the α_2-phase. Again, the relatively smooth surface of the mesomorphic α-phase regions underwent substantial morphologic changes caused by the shrinkage of the material during crystallization. The assignment of the mesomorphic and crystalline structures, which are observed in Figure 4a,b, to the β_2-phase and α_2-phases and the assignment of bright areas in Figure 4a to molten polymer are consistent with the changes accompanying the heating of the sample (Figure 4c). At elevated temperatures the long lamellae decomposed into parts, and the short lamellae became even smaller. Dark regions have also been reduced due to the partial isotropization of the mesomorphic α- and β-phases. On further heating, the image contrast related to the ordered structures gradually disappears.

The surface morphology of the bulk PDES-1, which has been slowly cooled from the melt to RT, is shown in Figure 5a,b. Most of the area consists of large flat domains, and only a few long lamellae are seen in the top part of the images. The lamellae are 300−400 nm in width, and most likely they are aggregates of thinner structures of the mesomorphic β-phase. In the result of crystallization, the large domains (as one seen in the central part of the images in Figure 5a,b) have been broken into smaller structures (a few microns in size)

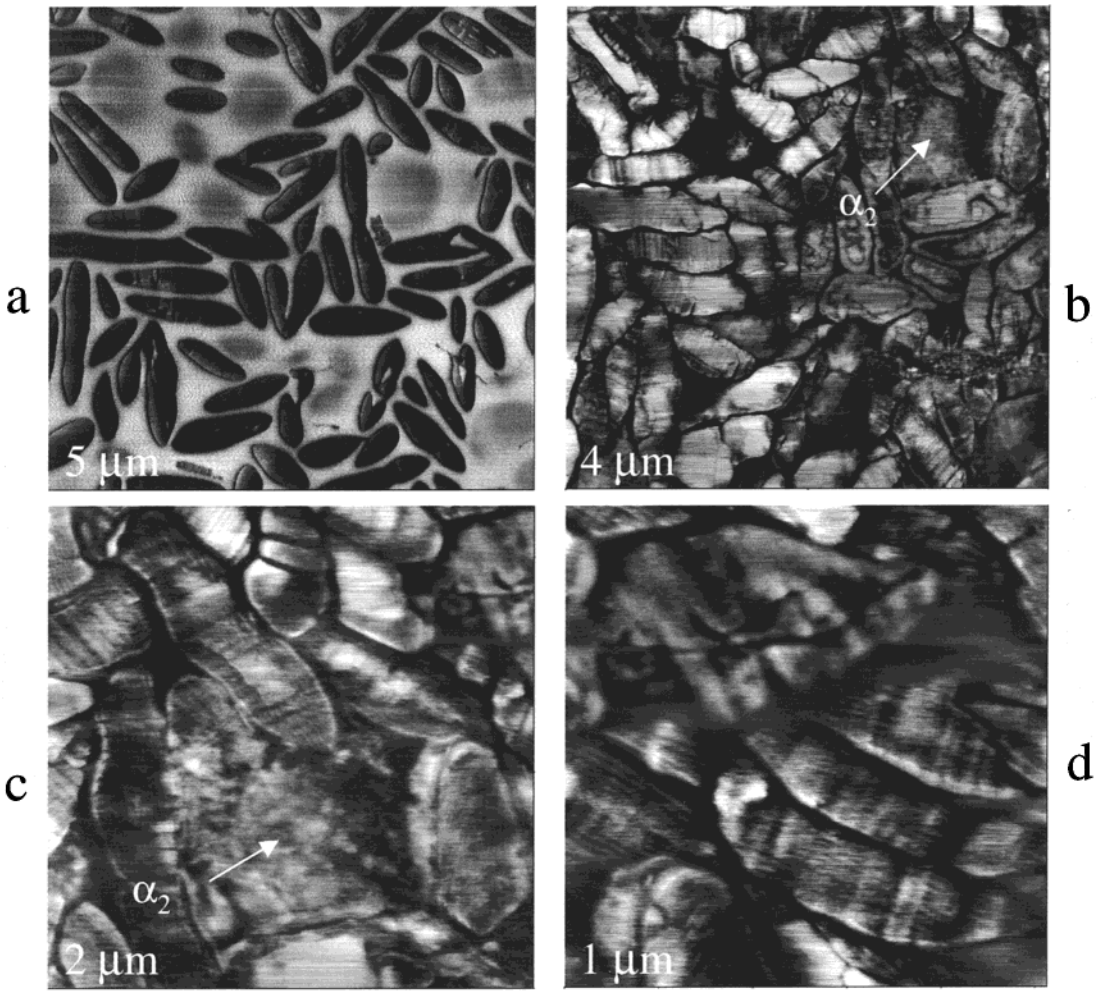

Figure 3. Phase images at the same location of the bulk PDES-2 sample (the same as in Figures 2) at RT (a) and after cooling to $T = -15$ °C (b). (c, d) Higher resolution phase images of the sample at $T = -15$ °C.

as seen in Figure 5c,d. The border of the large mesomorphic domain and the same location in the crystalline samples are indicated with broken white lines in the center of the images in Figure 5b,d. This process is accompanied by strong surface roughening. The corrugations of the crystalline surface are several times higher than of the mesomorphic surface. Morphologic changes observed during crystallization are reversible, and the large domains of the mesomorphic α-phase restore their shape on heating of the crystalline sample to RT.

Gradual changes of the polymer morphology and nanometer-scale structures, which occur during crystallization of the slowly cooled PDES-2 sample, are shown in Figure 6a−c. The phase image in Figure 6a shows a part of the area seen in Figure 2a, which was imaged at lower temperature ($T = -5$ °C). It is seen that crystallization of the α-mesophase is completed before the crystallization of the β-mesophase starts. The mesomorphic β-phase lamellae are seen bright in the left part of the image, whereas dark small domains, which are seen in the right part, can be assigned to the crystalline α_2-phase. On further cooling to $T = -10$ °C, most of the lamellae are broken into crystalline blocks, and only a few of them (e.g., three short lamellae in the central part of the image) remain in the mesomorphic state (Figure 6b). Note that crystallization of the large aggregate, which consists of several lamellae, led to the formation of multiple crystalline blocks. Further decreasing of the temperature to $T = -15$ °C is accompanied by complete crystallization of the rest of the β-mesomorphic structures (Figure 6c). Heating of the sample induces a gradual disappearance of crystalline morphology of both phases. Crystalline blocks of the β_2-lamellae become less pronounced, and some of the crystalline α_2-domains melt (Figure 6d). This process continues at higher temperatures, and the restoration of the mesomorphic morphology is followed by a complete isotropization of the sample in the vicinity of $T =$ 50 °C. It is important to emphasize that both α_2- and β_2-crystalline polymorphs transform to their own mesophases at the temperatures, which are very close to that indicated on the phase diagram (Figure 1). Our new finding consists of the fact that the isotropization temperature of the α-mesophase is slightly below that for β-mesophase.

3. Nanostructure of α- and *β*-Phases. Careful analysis of the images in Figure 6b−d shows that the surface of the crystalline lamellae exhibit fine striations, which are oriented along and perpendicular to their main direction. Also, some periodical structures can be found on the crystalline α_2-domains. These features are seen more distinctively in high-magnification phase images in Figure 7a−c. The images in Figure 7a,b show the bottom part of the three crystalline lamellae, which are surrounded by crystalline α_2-phase domains. The bright parts of the lamellae exhibit striations, which are oriented along their short direction, whereas striations

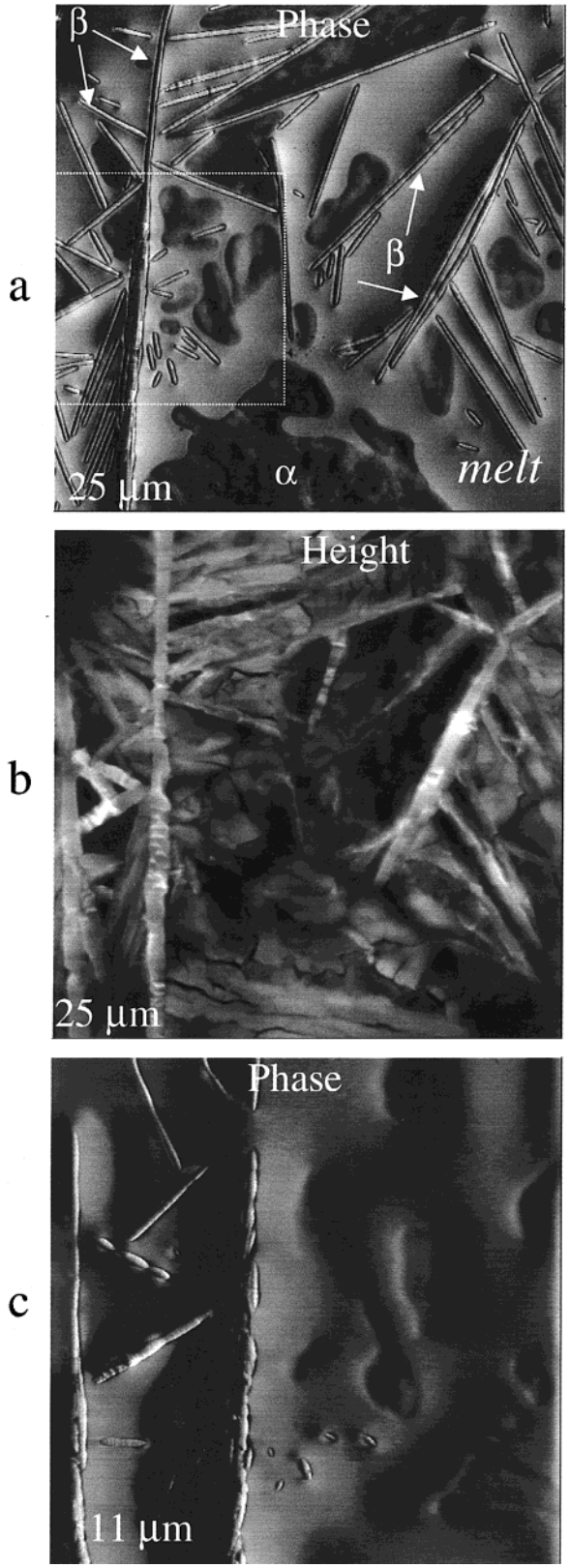

Figure 4. AFM phase and height images of the bulk PDES-2 sample recorded at different temperatures. (a) Surface of PDES-2 sample slowly cooled (~1 °C/min) from molten state (T = 100 °C) to RT. (b) The same location as in (a) after the slow cooling of the sample from RT to T = −15 °C. (c) The phase image of the surface location indicated by a dotted square in (a) after the sample was gradually heated (~0.5 °C/min) from T = −15 °C to T = 35 °C. In the height image (b) the contrast corresponds to surface corrugations in the 0−300 nm range. Different mesomorphic phases are indicated with "α" and "β".

along their long or main direction are seen in the dark parts of the lamellae. The latter striations are best resolved in Figure 7b, and they exhibit a repeat distance of ~25 nm. These structures are similar to those found in the images of the quenched PDES-2 samples (Figure 3c,d**)**. The crystalline α_2-phase domains also show bright striations with the repeat distance ~50 nm (Figure 7a). On heating, these nanostructures behave differently, and the image in Figure 7c shows only periodical features of the α_2-domains, whereas a piece of the lamellae, which is seen in the upper part, is featureless.

Periodical phase contrast variations in nanometer-scale reflect variations of local stiffness, which are directly related to chain packing. Well-ordered regions are typically seen bright and poorly ordered, darker.[37] Therefore, AFM observations of periodical nanometer-scale structures in the mesomorphic and crystalline phases are important for the understanding of PDES structures. Nanostructure of the mesomorphic β-phase lamellae is revealed in AFM images in Figure 8a−f. The height and phase images obtained in *light tapping* most correctly define the dimensions of the mesomorphic lamellae and the fine details of their surfaces (Figure 8a−c). A cross-section profile, which was taken along the horizontal direction marked with an arrow in the height image, shows that the height of these structures with respect to the amorphous surroundings is ~15 nm, and their width is ~300 nm. The bright contrast of the lamellae in the phase images indicates the higher stiffnesses as compared with their surroundings. If we suggest that half of the lamellae is above the amorphous level, then they can be characterized by a thickness-to-width ratio of 1:10. Slight striations along the width of the lamella, which are barely seen in the Figure 8a,b, are better resolved in the height image in Figure 8c. They are actually numerous steps of the surface layers as seen from this image and a cross-section profiles taken along the main direction of the lamella. In the cross-section profile, three surface steps, which are of 0.7−0.8 nm in height, are indicated with arrows. The step size is close to the cross-section dimensions of the crystalline PDES chains; therefore, we suggest that the surface of the mesomorphic lamellae is built up of multiple single layers of extended PDES chains.

Because PDES in the mesomorphic state is relatively soft, the AFM probe can deform such material and even penetrate through it as was shown in AFM images of the samples with rubbery-like surface layers.[34,38] Indeed, the AFM height image in Figure 8d, which was recorded in *hard tapping*, revealed nanostructure of the lamella different from that seen in the height image in Figure 6a. Bright striations extended along the main direction are seen in all lamellae. The separation distance between them varies in the 80−120 nm range. A cross-section profile, which was taken across the image, shows that the AFM probe substantially deforms the amorphous surroundings and also some mesomorphic material. The pronounced peaks of this profile (two side peaks are indicated with arrows) correspond to more rigid linear nanostructures, whereas the mesomorphic material around them is depressed by the probe. When the tip force was reduced, the height image and the similar profile changed substantially (Figure 8e). First, surface corrugations of the mesomorphic lamellae and neighboring amorphous regions become much smaller. Second, the rigid linear nanostructures, which are marked with arrows, are seen lower than the

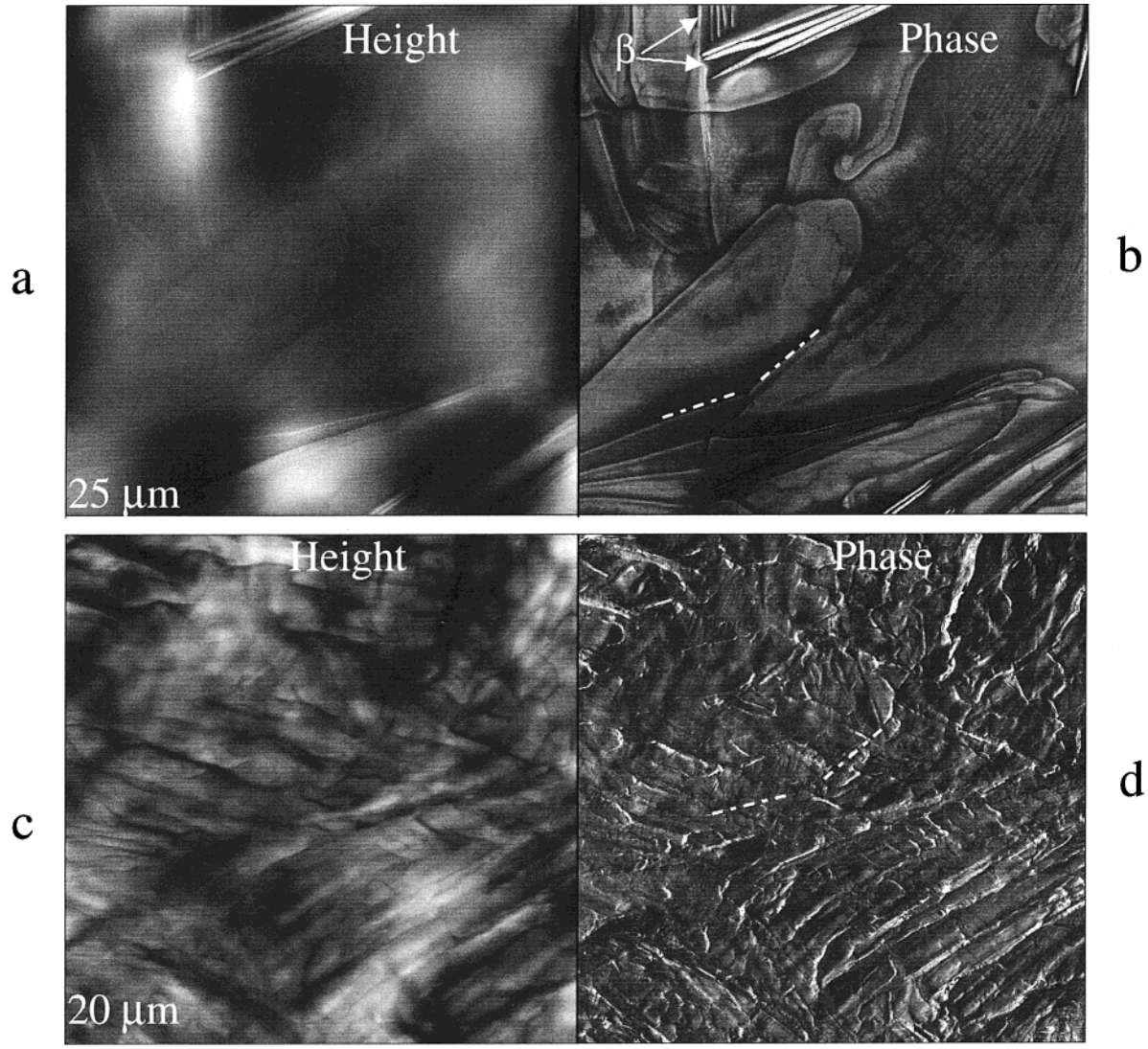

Figure 5. Height and phase images of a surface of bulk PDES-1 sample, which was prepared by the slow cooling from molten state (T = 100 °C) to RT. Images a and b were obtained at RT and images c and d after cooling to T = −15 °C. The contrast in height images covers surface corrugations in the 0−200 nm range in (a) and in the 0−1200 nm range in (c). In the phase images b and d the edge of the same domain is indicated with white dotted lines. In image b, the lamellae of the β-phase are marked as "β".

immediate surrounding. Most likely, the mesomorphic material, which was depressed in *hard tapping*, recovered and started a buildup of a more equilibrium structure that was disturbed by the probe. This is confirmed by the image in Figure 8f, which was recorded at the same location after 2 h of recovery. The cross-section profile of this image becomes much closer to the one shown in Figure 8a. Also, the linear nanostructures, which were present in Figure 8d,e, are no longer seen. Instead, contrast variations show a growth of multiple surface layers common for the nondisturbed lamellae.

AFM visualization of molecular surface layers and the subsurface "skeleton" consisting of rigid extended nanostructures was achieved not only on relatively short lamellae but also on extended lamellae. Figure 9a,b shows height images of part of a long mesomorphic lamellae of the slowly cooled PDES-2, which were obtained in *light* and *hard tapping*, respectively. In the first image one sees four parallel lamellae with fine surface features corresponding to their multilayered surface structure, which are separated by amorphous regions. A cross-section profile shows the lamellae's curved shapes, which elevate 10−20 nm above the amorphous level. Striped patterns with the repeat distance of ∼90 nm, which are seen on these lamellae in the *hard tapping*, define their rigid skeletons. The corresponding cross-section profile reflects variations of local stiffness with amorphous material between the lamellae being depressed most strongly. The tip-induced surface modification is distinctive in the phase image (Figure 9c), which was recorded immediately after the image in Figure 9b. The rectangular patterns seen in this image indicates the area, which was scanned in *hard tapping*. This modification has disappeared after several hours.

B. Morphology of Shear-Induced PDES Layers. Mesomorphic PDES, similar to other liquid crystalline polymers, can be oriented by shearing.[2] We used this approach to produce oriented layers of PDES on Si substrate by rubbing. Such procedures are often applied for preparation of polymer surfaces with oriented structures.

1. Thick Layers. First, we examined AFM images obtained on thick layers of PDES-1 and PDES-2 shown in Figure 10a−d. The height image, which was recorded on an oriented PDES-2 layer at RT, reveals multiple

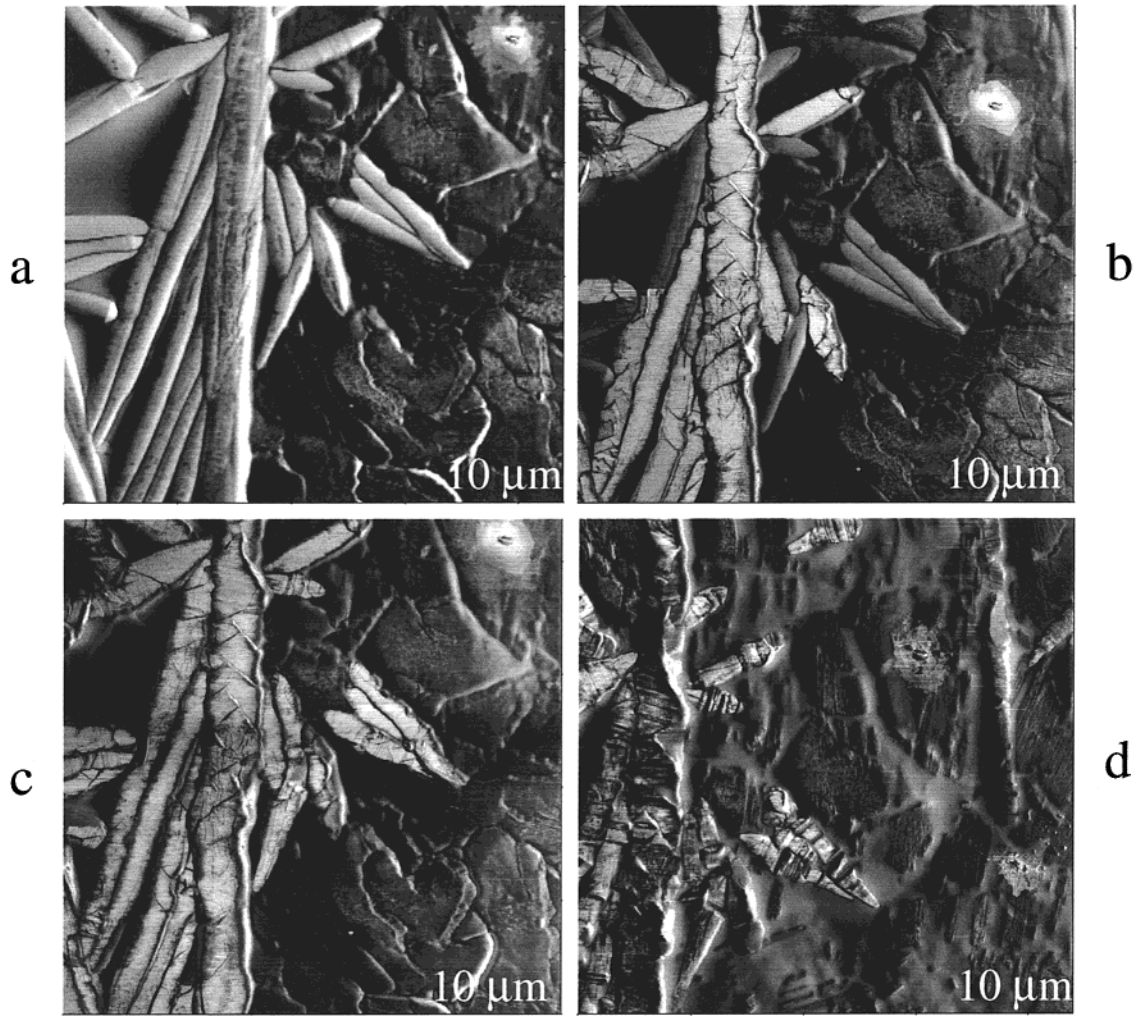

Figure 6. AFM phase images of slow cooled PDES-2 sample (the same as in Figure 4) at temperatures $T = -5$ °C (a), $T = -10$ °C (b), $T = -15$ °C (c), and $T = +15$ °C (d).

β-mesomorphic lamellae. The lamellae are ~420 nm wide, and they are elongated perpendicular to the rubbing direction. Patches of amorphous polymer are seen between the neighboring lamellae. Crystallization of this samples is accompanied by drastic morphologic changes, and crystalline blocks, similar to those found earlier in PE extended chain lamellae,[30,31] dominate in the image obtained at $T = -15$ °C (Figure 10b). The width of these crystalline blocks is ~600 nm which is a consequence of crystallization of mesomorphic lamellae and the nearby amorphous material. Some crystalline blocks include two or more neighboring lamellae. Nanoscale striations, which are oriented along the rubbing direction, are seen on the surface of the crystalline blocks. Elongated lamellae of the mesomorphic and crystalline β_2-phase of the oriented PDES-1 sample are shown in Figure 10c,d. After crystallization the individual lamellae retain their dimensions, and multiple crystalline blocks are observed within the lamellae. The width of the PDES-1 lamellae (~250 nm) is smaller than that of the PDES-2 sample which reflects the different molecular weight of these polymers and the extended character of the polymer chains in the lamellae.

The described lamellar morphology undergoes reversible changes during cooling and heating cycles. The main distinct change in the structure of the single crystalline lamellae during melting and transformation to the mesomorphic state is the disappearance of blocks with linear substructures oriented along the rubbing direction. The width of the individual mesomorphic lamellae just after the melting of the β_2-crystalline phase is very close to the width of the single crystalline lamellae. Upon further heating, in some places the mesomorphic lamellae became narrower (Figure 10c), which seems to be a result of initiation of their surface isotropization. We observed that the lamellae induced by rubbing are less equilibrium than the β-mesomorphic lamellae obtained by slow cooling and even by quenching. Also in AFM imaging in *hard tapping*, the probe interacting with the lamellae might change their orientation and damage them.

2. Thin Layers. The described morphology is common for PDES layers with a thickness of about 1 μm. When the thickness of the layer becomes smaller (in the 200−300 nm range), structural organization of the polymer can be influenced by the nature of the substrate. Indeed, thin PDES-1 layers wet the Si substrate, which was treated by Ar^+ plasma, much better that the nontreated Si. As a result, the PDES-1 layer completely coats the modified Si substrate (Figure 11a), and its morphology is characterized by blocks of mesomorphic lamellae embedded in amorphous polymer. The lamellae are lying perpendicular to the rubbing direction. Rubbing of PDES-1 on the unmodified Si substrate results in isolated patches and droplets of the polymer.[35,37]

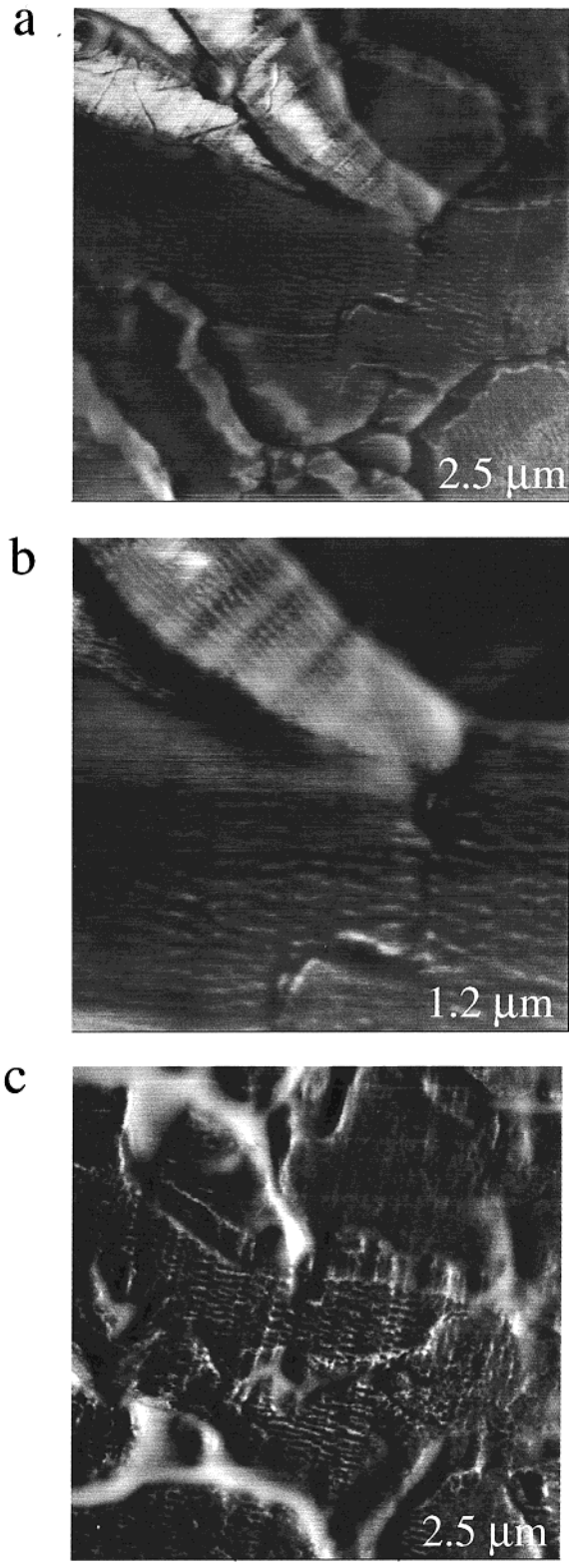

Figure 7. High-magnification AFM phase images of the slow cooled PDES-2 sample at $T = -15$ °C (a, b) and $T = +10$ °C (c).

Crystallization of the rubbed mesomorphic lamellae starts upon cooling below $T = -5$ °C and is manifested by a sharp change in the surface structure (Figure 11b). Crystalline blocks (hundreds of nanometers in size) with distinctive edges are formed from the mesomorphic material. Some of the blocks similar to those formed in thick layers (Figure 10b) can incorporate material from several neighboring mesomorphic lamellae. After crystallization of the β-mesomorphic lamellae, amorphous areas became smaller, reflecting incorporation of some material into crystalline blocks. The amorphous material remaining in between the crystalline aggregates (see left part of the image in Figure 11b) at $T = -10$ °C is a direct consequence of the strong local interaction of the thin layer with the plasma-treated substrate, i.e., its confined geometry.

This amorphous material crystallized at a lower temperature ($T = -25$ °C) with the formation of tiny fibrils (20−30 nm in thickness) bridging two neighboring crystalline domains (Figure 11c,d). In these images one sees that the fibrils emerge out of crystalline blocks being an extension of their skeleton. The top layers of the lamellae shrink upon cooling leaving the edges of the skeleton uncovered. They can further extend by adding the outside amorphous material in the low-temperature crystallization. This description is consistent with the presence of surface regions with cross-hatched structures in the crystalline material (Figure 11c,d). Nanometer-scale features of the top surface of crystalline lamellae, which are extended along the rubbing direction, intersect with the fibrils of the lamella skeleton, which are aligned perpendicular to the rubbing direction. All these features are common for the crystalline β_2-phase lamellae and blocks (Figures 3c,d and 7a,b**)**.

On melting, the crystalline morphology of thin PDES layers changes in a two-stage process. First, the fibrilar structures grown in secondary crystallization have disappeared ($T = -5$ °C). At higher temperatures, crystalline blocks are transformed into mesomorphic lamellae. This process is completed at $T = +16$ °C, in good agreement with the melting temperature of the crystalline β_2-phase (Figure 1).

In other experiments, we have checked the influence of the substrate on isotropization of the mesomorphic structures observed in thin PDES-1 films. Figure 12a−c demonstrates a step-by-step isotropization of the thin mesomorphic layer, which occurs as a result of the surface melting of the lamellae. The lamella skeleton disappears as seen in Figure 12c. After heating this sample to 43 °C, there were no traces of the lamellar morphology detectable in the AFM images. This result correlates with the isotropization temperature of the bulk PDES-1 at $T = 47$ °C obtained by DSC.[6]

Cooling of the sample after a short time annealing at $T = 43$ °C led to the morphology changes documented in Figure 12d−f. Mesomorphic lamellae have appeared again in the vicinity of RT, and their preferential orientation (perpendicular to the initial rubbing direction) was preserved yet the lamellae became more elongated than in the initial ones (Figure 12d). This indicates an incomplete isotropization in the sample heated to $T = 43$ °C. The mesomorphic lamellae, induced by cooling, resemble the lamellae in the thick layer (Figure 10c). The width of the elongated mesomorphic lamellae is in the 200−250 nm range, and some of them merge together to form wider platelets. On the surface of the lamellae, there are striations perpendicular to the main lamellae direction, and they are similar to those seen on the surface of mesomorphic lamellae of bulk PDES (Figure 8a−c**)**. Upon crystallization, the mesomorphic lamellae are broken into small blocks, which form the mosaic structure of the crystalline lamellae. The shape and dimension of the crystalline lamellae are quite analogous to the crystalline lamellae in thick

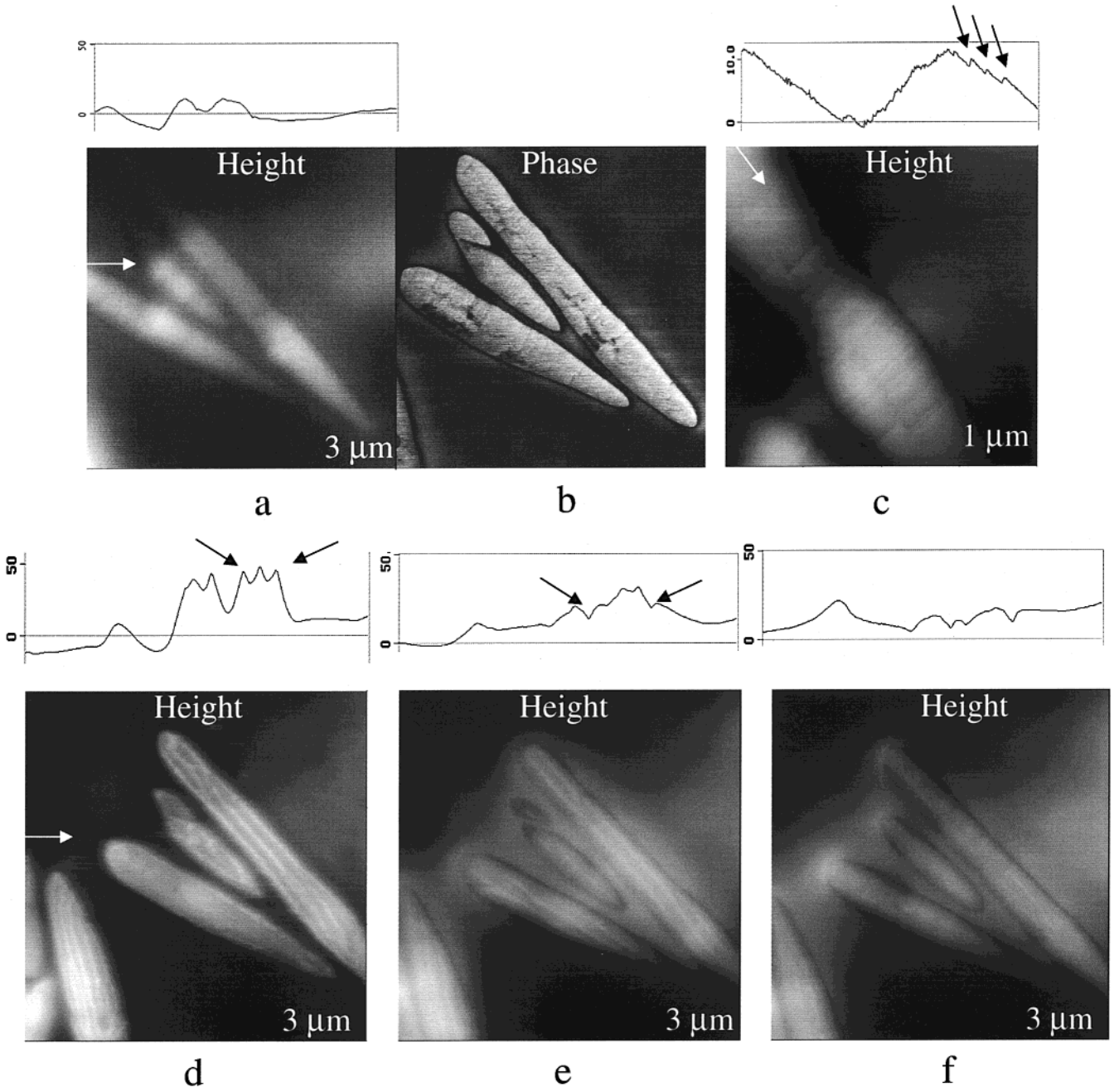

Figure 8. AFM height and phase images of mesomorphic β-phase of the slow cooled PDES-2, which were obtained at RT at different tip−sample force interactions. Images in (a), (b), and (c), light tapping; image in (d), hard tapping. Image in (e) was obtained in light tapping immediately after the image in (b). Image in (f) was obtained in light tapping 3 h after the image in (b). Cross-section profiles (0−10 and 0−50 nm scales), which are shown above the height images (c−f), were recorded along the directions indicated by arrows.

layers (Figure 10d). High-resolution images (not shown here) reveal nanostructure of the crystalline lamellae, which is similar to what was discussed above (Figures 7a and 10b).

In addition to the mesomorphic and crystalline β-phase structures (there are no traces of the mesomorphic and crystalline α-phases) observed in the thin PDES-1 film at temperatures down to $T = -20$ °C, large surface areas are covered with amorphous material. At further cooling, this amorphous material crystallized but differently than the confined amorphous regions seen in Figure 11b. At temperatures below −20 °C, we observed a formation of spherulite-like structures in previously amorphous regions (Figure 12f, the right low corner). They can be assigned to the crystalline α-phase structures, which might incorporate all amorphous material upon further cooling. Some bundlelike structures composed of tiny fibrils were grown at the edges of the crystalline β-lamellae, and they are similar to the fibrils seen in Figure 11c,d.

Summary

Visualization of the mesomorphic and crystalline structures of different PDES samples with AFM provided unique capabilities for better understanding its phase diagram and nanoscale architecture.

Phase Behavior of PDES As Revealed from AFM. In studies of multiphase polymers AFM allows examination of the sample heterogeneity on the micron

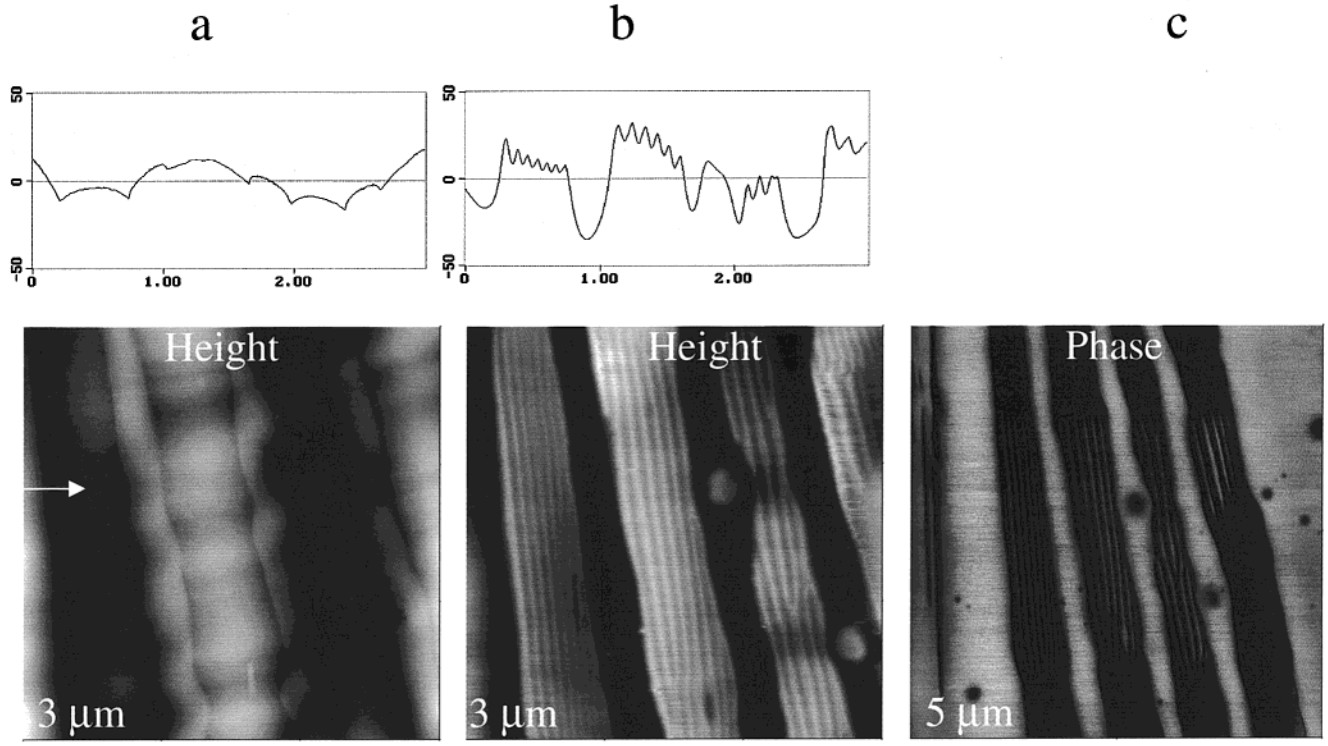

Figure 9. AFM height images of the mesomorphic β-phase structures of the slowly cooled PDES-2, which were obtained in light tapping (a) and in hard tapping (b). Cross-section profiles (0−50 nm scale), which were taken along the direction indicated with an white arrow, are shown above the height images. (c) Phase image obtained in light tapping on the area, which includes the surface location imaged in hard tapping (b).

and submicron scale. In PDES samples, the image contrast differentiates surface regions of amorphous material and the α- and β-phase structures, all of them having different densities. Also, the characteristic shape of the structures can help to identify various phases. Morphologic changes, which have been recorded in the AFM images at different temperatures, correlate with temperatures of the thermal transitions determined by DSC and other methods. The fact that structures seen in images of bulk samples, thick and thin layers of PDES and PDPS,[39] in ultrathin films of PDPS[40] other mesomorphic polysiloxanes[37] are quite similar indicates that surface morphology reasonably well reflects overall sample morphology.

The important result obtained is the identification of two different morphologies in the crystalline and mesomorphic PDES phases. The phase diagram of PDES, which was based on the X-ray and calorimetric data,[6,7] suggests that the crystalline α- and β-polymorphs transform after melting to a single mesophase. Yet, our results revealed two different mesomorphic phases. The mesomorphic β-phase is characterized by the elongated lamellar structures, whereas the characteristic morphology of the mesomorphic α-phase is the domains. Therefore, question marks which are seen in the mesomorphic frame in Figure 1 can be removed. There are definite consequences of this finding. For example, results of X-ray diffraction, calorimetric, NMR, and other experiments on isotropization of the mesomorphic state of PDES required reconsideration and more careful examination to clarify the contribution of different mesomorphic phases. In DSC experiments it was shown that two factors are important for the shape (single, double, or sometimes multiple) and the broadness of the isotropization peak. Namely, the broadness of the molecular weight distribution and the sample's thermal history are factors of primary importance for the isotropization process. Now it becomes obvious that the thermal history influences primarily the ratio between α- and β-PDES in both the crystalline and mesomorphic states.

Typically α- and β-PDES coexist in the sample. The ratio between the crystalline polymorphs is easy to estimate on the basis of the well-defined differences in the melting points and heat of fusion of the α- and β-polymorphs.[6−8] Similar identification needs to be done for the α- and β-mesomorphic PDES. Because of the small values of the heat of isotropization (3−4 J/g), it is a more difficult task. AFM visualization of the mesophase morphology may be the most direct method of estimation of the content of coexisting α- and β-PDES.

Shearing of PDES into layers induces a formation of predominantly mesomorphic β-phase. Morphologic studies of thin PDES layers on the modified Si substrate showed that the mesophase formation and crystallization in such layers may be prohibited considerably due to constrained geometry and interaction with the solid surface. In the constrained geometry the molten layers may crystallize directly from the amorphous melt without intermediate transformation to the mesophase.

Mesomorphic Lamellae of β-PDES. High-resolution imaging of the mesomorphic PDES structures with optical and electron microscopy[6,32] has definite limitations, which can be overcome with AFM. In most AFM images the lamellae, which are characteristic for the β-phase, are seen surrounded by amorphous polymer. Individual lamella has an anisotropic shape with the width being much larger than the thickness. This was found in AFM imaging at elevated forces on the bulk PDES samples, thin and ultrathin films.[39] In other words, the mesomorphic lamellae are lying flat with respect to the surface. There is a definite, but a not

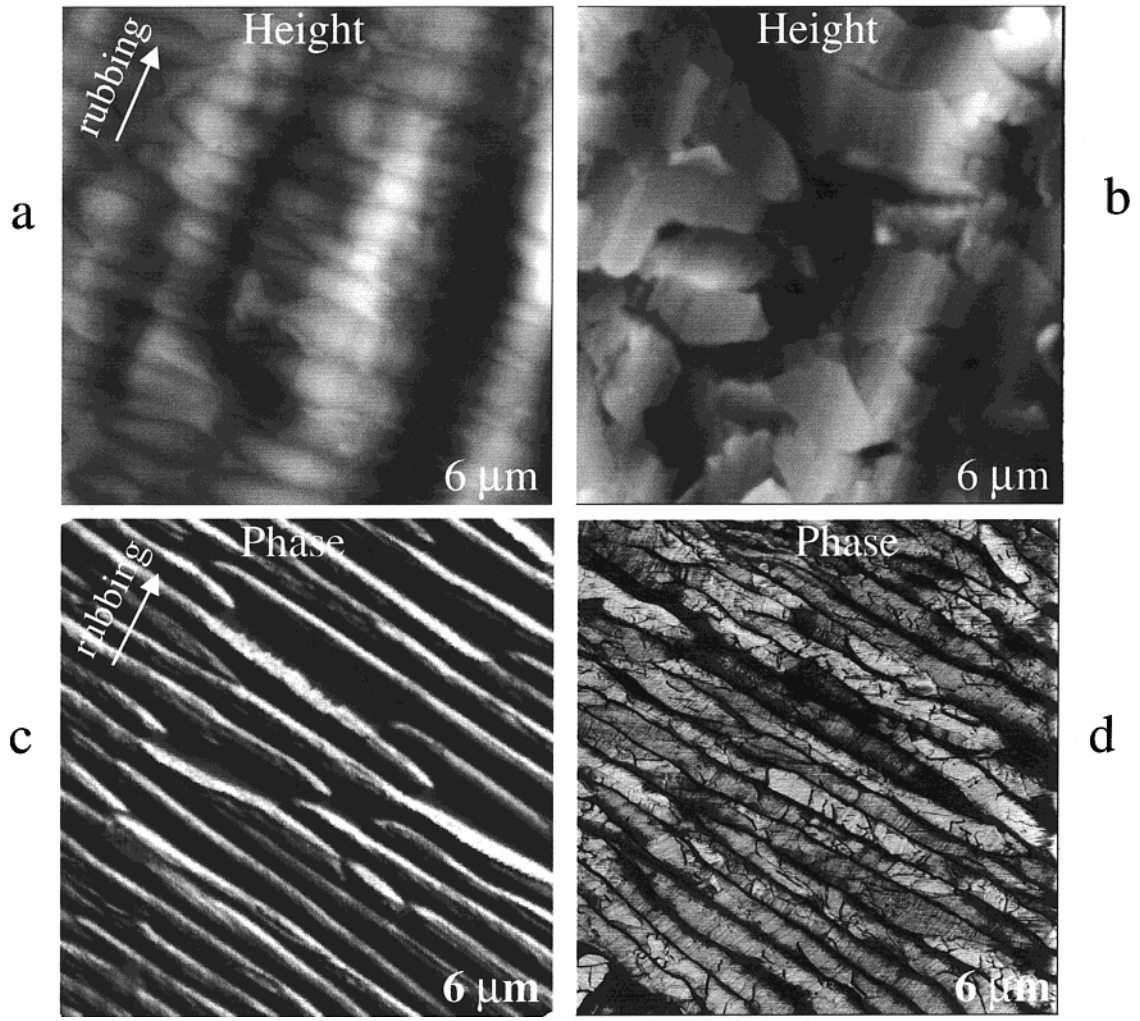

Figure 10. Height and phase images of thick oriented layers of PDES-2 (a, b) and PDES-1 (c, d) measured at different temperatures. Images in (a, c) were obtained at RT and images in (b, d) at $T = -15$ °C. The contrast in height images corresponds to surface corrugations in the 0−150 nm range in (a) and in the 0−350 nm range in (b).

Table 2. Length of the Extended Crystalline PDES Chains and the Thickness of the Crystalline and Mesomorphic Lamellae Estimated from AFM Images

sample and preparation	completely extended chain L,[a] nm	width of lamellae of β-PDES, nm	
		crystalline	mesophase
PDES-1 (slow cooling)	226	275 ± 50	275 ± 50
PDES-2 (slow cooling)	1026	600 ± 100	600 ± 100
PDES-1 (quenched)	226	180 ± 30	100 ± 30
PDES-2 (quenched)	1026	300 ± 30	170 ± 30
PDES-1 (shear induced)	226	250 ± 30	250 ± 30
PDES-2 (shear induced)	1026	600 ± 100	420 ± 100

[a] Length (L) of a completely extended PDES chain of molecular weight M_n was estimated from the following equation: $L = (c/2)(M_n/M_0)$, where $c = 0.475$ nm is the length along the chain axis of a unit cell containing two monomer units,[7] and $M_0 = 102.2$ is the molecular weight of the monomer unit.

complete, correlation between the width of the lamellae in the mesomorphic and crystalline state and the length of extended chains in PDES samples with different molecular weight (Table 2). The fact that the width of mesomorphic lamellae is smaller than the length of the fully extended PDES chains does not contradict earlier suggestions[8,17,26,32] that the thickness of the β-PDES lamellae correlates with the length of the extended chain conformation. The situation becomes clear from the consideration of the complex structure of the individual lamellae, which is shown in Figure 13a. This image presents a 3D view of the mesomorphic lamellae, which has not been visualized so far. Only large aggregates of the mesomorphic lamellae were observed with optical and electron microscopies.[17] AFM imaging of the mesomorphic lamellae in *light* and *hard* tapping allows us to suggest its structural model (Figure 13b). A skeleton, which consists of fibrils 20−30 nm in width, is hidden inside of the lamellae being wrapped by numerous monomolecular layers of extended chains. Surface steps, which are seen on the lamella surface, correspond to the interchain distance of ∼0.8 nm determined for crystalline PDES with X-ray diffraction. Most of the extended chains are oriented along the short axis of the lamellae (as suggested from optical microscopy data[17]) and can curve over the lamella edges.

So far in the literature discussion of extended chain morphology of mesomorphic polysiloxanes was based on the concept of crystal growth through a transient mobile phase.[8] This concept was first suggested for explanation of crystallization of the hexagonal phase of PE under high pressure and lately extended to crystallization of some flexible polymers via preliminary mesophase formation (see, for example, refs 4, 5, 29, and 30). It was suggested that initial ordering of the mesophase proceeds in the chain-folded form followed by lamellae thickening via rapid chain extension through the sliding of macromolecules along each other. In general, the

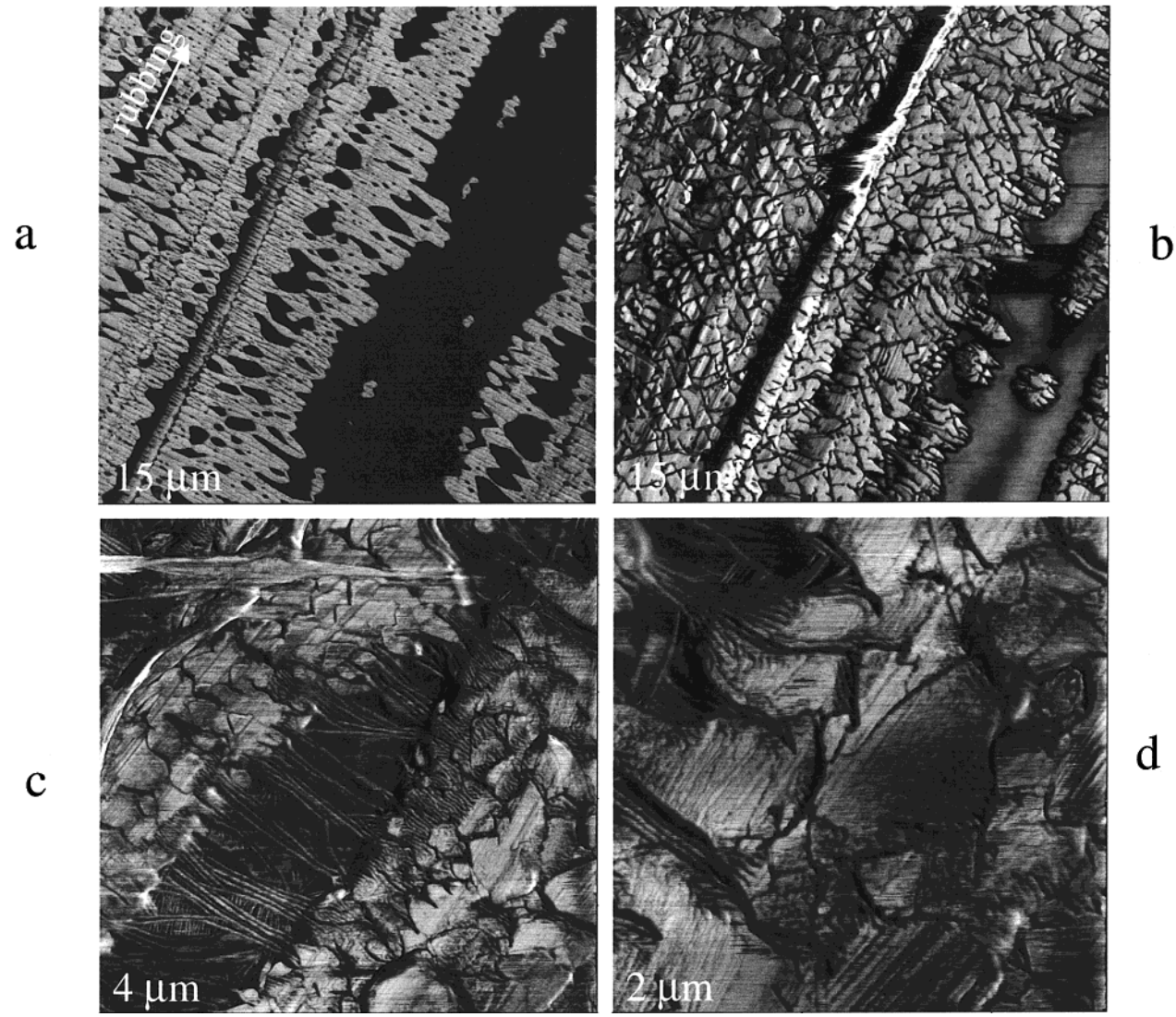

Figure 11. AFM phase images of a thin oriented PDES-1 layer on a plasma-treated Si wafer at RT (a) and at $T = -6$ °C (b). High-resolution phase images in (c) and (d) were obtained at $T = -40$ °C.

complex structure of the mesomorphic PDES lamellae does not contradict the concept but shows a need in its more detailed development. We might assume that the fibrils of the skeleton are actually chain-folded structures, and the length of the skeleton is related to crystallization conditions. The latter, however, does not influence the overall architecture because the monomolecular layers have been observed on all PDES lamellae independent of their length. Also, the amount of polymer material involved in the formation of the skeleton and the overlayers can be different for polysiloxanes of different chemical nature, and this can result in variations of their crystallinity.

Mesomorphic and Crystalline α-PDES. Besides the crystalline and mesomorphic β-phase lamellae, we observed domains of different size, which have been assigned to the α-PDES structures in the mesomorphic and crystalline state. In the samples with a low amount of the β-phase, the mesomorphic α-PDES domains have dimensions of tens of microns, and during crystallization the domains are broken into smaller micron-size blocks. Similar crystalline α-phase structures have been observed in TEM micrographs.[8,9] In the samples where α-PDES and β-PDES coexist in comparable portions, the dimensions of the α-PDES domains may be smaller due to restrictions resulting from the presence of β-PDES lamellar structures. High-resolution images of the α-phase domains only in a few cases reveal ordered structures with a repeat distance of 50−60 nm. This result in combination with density data for the crystalline α_2-phase indicates an inferior chain order in this phase as compared to the β-phase.

The situation with the chain conformations in the α-phases is more complex. X-ray, DSC, and NMR show[1,2] that the degree of crystallinity of the α-PDES is normally as high (≥90%) as that for the β-PDES where, as we saw above, the extended chain conformations dominate. It has been suggested that PDES chains in the α-crystals are extended; however, they contain a large number of defects such as kinks and nonsegregated chain ends, which may be incorporated into the crystalline regions. This might cause an overlapping of the chains and formation of continuous domains that are observed in AFM images. It is worth noting that the crystalline α- and β-phases of bulk PDES samples do not exhibit spherulitic morphology that according to the modern viewpoint is a consequence of chain folding.[41] This is another indication of the extended chain arrangements in these phases.

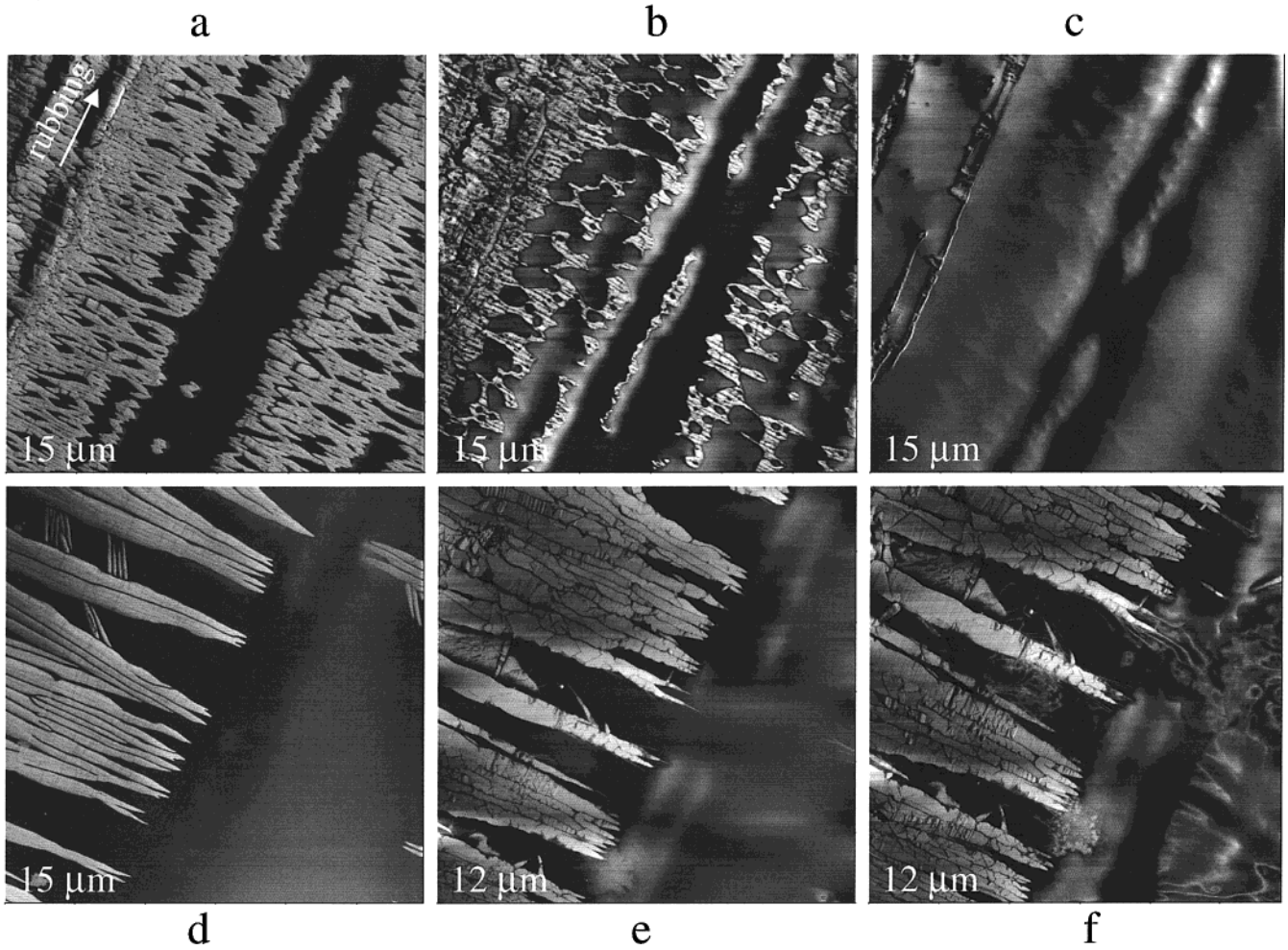

Figure 12. AFM phase images of a thin oriented PDES-1 layer on a plasma-treated Si wafer, which was obtained at different temperatures. (a) RT, (b) $T = 32$ °C, (c) $T = 40$ °C, (d) $T = -6$ °C, (e) $T = -13$ °C, and (f) $T = -26$ °C.

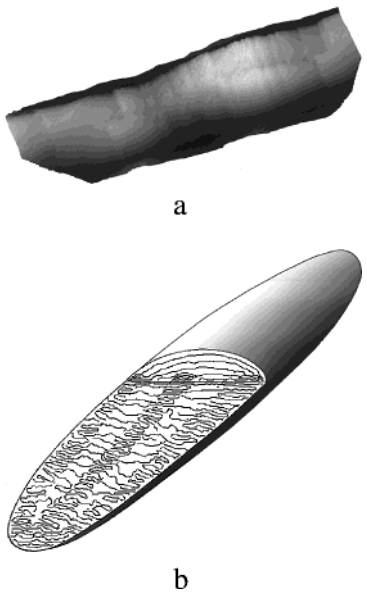

Figure 13. (a) AFM 3D view of the mesomorphic lamellae of β-PDES. (b) Structural model of the lamella. A part of the lamellae is removed to show the 20−30 nm wide fibrils inside the lamellae. They might be formed by partially folded polymer chains.

Finally, one of the issues that motivated the present study is concerned with the effect of the molecular weight on PDES morphology. The good correlation between the lamellar thickness as estimated from AFM for the PDES-1 of various thermal treatments and the calculated chain length has confirmed the extended chain conformation for β-PDES in both mesomorphic and crystalline states. For the significantly high molecular weight PDES-2 lamellae thickness for β-PDES is considerably lower than expected from the calculation. This may be attributed to the influence of kinetic effects and a complex morphology of the lamellae (Figure 13). It is important to mention that a similar effect of the molecular weight has been revealed for the same PDES-2 sample in the TEM study.[8,9] Because of the absence of distinct lamellae for α-PDES, no direct influence of the molecular weight on morphology of PDES-2 has been found for the α-PDES.

Acknowledgment. We thank Prof. Martin Moeller (Ulm University, Germany) for his helpful discussions. Yu.K.G. is also thankful to Digital Instruments Inc. and the University of California, Santa Barbara (Prof. E. Kramer), for support of his research visits, during which this AFM study was performed. This work (V.S.P.) was partly supported by RFBR (Grant 98-03-33329).

References and Notes

(1) Godovsky, Y.; Papkov, V. *Adv. Polym. Sci.* **1989**, *88*, 129.
(2) Molenberg, A.; Moeller, M.; Sautter, E. *Prog. Polym. Sci.* **1997**, *22*, 1133.
(3) Wunderlich, B.; Grebovich, J. *Adv. Polym. Sci.* **1984**, *60/61*, 1.

(4) Wunderlich, B.; Moeller, M.; Grebovich, J.; Baur, H. *Adv. Polym. Sci.* **1988**, *87*, 1.
(5) Ungar, G. *Polymer* **1993**, *34*, 2050.
(6) Papkov, V.; Godovsky, Y.; Svistunov, V.; Litvinov, V.; Zhdanov, A. *J. Polym. Sci., Polym. Chem. Ed.* **1984**, *22*, 3617.
(7) Tsvankin, D.; Papkov, V.; Zhukov, V.; Godovsky, Y.; Svistunov, V.; Zhdanov, A. *J. Polym. Sci., Polym. Chem. Ed.* **1985**, *23*, 1043.
(8) Molenberg, A.; Moeller, M. *Macromolecules* **1997**, *30*, 8332.
(9) Molenberg, A. Thesis, University of Ulm, Germany, 1997.
(10) Beatty, C.; Pochan, J.; Froix, M.; Hinman, D. *Macromolecules* **1975**, *8*, 547.
(11) Beatty, C.; Karasz, F. *J. Polym. Sci., Polym. Phys. Ed.* **1975**, *13*, 971.
(12) Pochan, J.; Beatty, C.; Hinman, D. *J. Polym. Sci., Polym. Phys. Ed.* **1975**, *13*, 977.
(13) Litvinov, V.; Lavruchin, B.; Papkov, V.; Zhdanov, A. *Dokl. Akad. Nauk* **1983**, *271*, 900.
(14) Godovsky, Y.; Papkov, V. *Macromol. Chem. Makromol. Symp.* **1986**, *4*, 71.
(15) Shulgin, A.; Godovsky, Y. *Polym. Sci. USSR* **1987**, *29*, 2845.
(16) Friedrich, J.; Rabolt, J. *Macromolecules* **1987**, *20*, 1975.
(17) Papkov, V.; Svistunov, V.; Godovsky, Y.; Zhdanov, A. *J. Polym. Sci., Polym. Phys. Ed.* **1987**, *25*, 1859.
(18) Papkov, V.; Kvachev, Y. *Prog. Colloid Polym. Sci.* **1989**, *80*, 221.
(19) Varma-Noir, M.; Wesson, J.; Wunderlich, B. *J. Therm. Anal.* **1989**, *35*, 1913.
(20) Koegler, G.; Laufakis, K.; Moeller, M. *Polymer* **1990**, *31*, 1538.
(21) Out, G. Ph.D. Dissertation, University of Twente, Enschede, The Netherlands, 1994.
(22) Godovsky, Y.; Makarova, N. *Philos. Trans. R. Soc. London, A* **1994**, *A234*, 45.
(23) Out, G.; Turetskii, A.; Moeller, M.; Oelfin, D. *Macromolecules* **1995**, *28*, 596.
(24) Turetskii, A.; Out, G.; Klok, H.; Moeller, M. *Polymer* **1995**, *36*, 1303.
(25) Shulgin, A.; Godovsky, Y.; Makarova, N. *Thermochim. Acta* **1994**, *238*, 337.
(26) Slottke, H. Thesis, University of Mainz, Germany, 1995.
(27) Litvinov, V.; Whittaker, A.; Hagemayer, A.; Spiss, H. *Colloid Polym. Sci.* **1989**, *267*, 1989.
(28) Grinberg, F.; Kimmich, R.; Moeller, M.; Molenberg, A. *J. Chem. Phys.* **1996**, *105*, 9657.
(29) Wunderlich, B. *Macromolecular Physics*; Academic Press: New York, 1973; Vol. 1.
(30) Barhem, P. Crystallization and Morphology of Semicrystalline Polymers. In Cahn, W., Haasen, P., Kramer, E. J., Thomas, E. L., Eds.; *Materials Science and Technology*; VCH Publishers: New York, 1993; Vol. 12.
(31) Keller, A.; Hikosaka, M.; Rastogi, S.; Toda, A.; Barham, P. J.; Goldbeck-Wood, G. In *Self-Order and Form in Polymeric Materials*; Keller, A., Warner, M., Windle, A. H., Eds.; Chapman & Hall: London, 1995; pp 1−15.
(32) Obolonkova, E.; Papkov, V. *Vysokomol. Soyed.* **1990**, *B31*, 691.
(33) Sheiko, S. S. *Adv. Polym. Sci.* **2000**, *151*, 61.
(34) Magonov, S. N. Atomic Force Microscopy in Analysis of Polymers. In *Encyclopedia of Analytical Chemistry*; Meyers, R. A., Ed.; John Wiley & Sons Ltd.: Chichester, 2000; pp 7432−7491.
(35) Magonov, S.; Elings, V.; Papkov, V. *Polymer* **1997**, *38*, 297.
(36) Magonov, S. N.; Reneker, D. H. *Annu. Rev. Mater. Sci.* **1997**, *27*, 175.
(37) Magonov, S. N.; Godovsky, Yu. K. *Am. Lab.* **1998**, *30*, 15.
(38) Magonov, S. N.; Godovsky, Yu. K. *Am. Lab.* **1999**, *31*, 52.
(39) Godovsky, Yu. K.; Magonov, S. N.; Papkov, V. S. Manuscript in preparation. In imaging of the PDES films prepared by spin-casting of a dilute polymer solution, we have observed elongated lamellae lying directly on the substrate, and its height has been at least 10 times smaller than the width.
(40) Godovsky, Yu. K.; Magonov, S. N.; Papkov, V. S. Manuscript in preparation.
(41) Basset, D. C. *J. Macromol. Sci., Phys.* **1999**, *B38* (5&6), 479.

MA000845V